A STRONGLY MAGNETIZED PULSAR WITHIN GRASP OF THE MILKY WAY'S SUPERMASSIVE BLACK HOLE

N. Rea 1 , P. Esposito 2 , J. A. Pons 3 , R. Turolla 4,5 , D. F. Torres 1,6 , G. L. Israel 7 , A. Possenti 8 , M. Burgay 8 , D. Viganò 1,3 , A. Papitto 1 , R. Perna 9 , L. Stella 7 , G. Ponti 10 , F. K. Baganoff 11 , D. Haggard 12 , A. Camero-Arranz 1 , S. Zane 5 , A. Minter 13 , S. Mereghetti 2 , A. Tiengo 2,14,15 , R. Schödel 16 , M. Feroci 17 , R. Mignani 2,5,18 , D. Götz 19

Draft version September 9, 2013

ABSTRACT

The center of our Galaxy hosts a supermassive black hole, Sagittarius (Sgr) A*. Young, massive stars within 0.5 pc of Sgr A* are evidence of an episode of intense star formation near the black hole a few Myr ago, which might have left behind a young neutron star traveling deep into Sgr A*'s gravitational potential. On 2013 April 25, a short X-ray burst was observed from the direction of the Galactic center. Thanks to a series of observations with the Chandra and the Swift satellites, we pinpoint the associated magnetar at an angular distance of $2.4 \pm$ 0.3 arcsec from Sgr A*, and refine the source spin period and its derivative (P = 3.7635537(2)) s and $\dot{P} = 3.7635537(2)$ s and $\dot{P} = 3.7635537(2)$ s $6.61(4) \times 10^{-12} \,\mathrm{s\ s^{-1}}$), confirmed by quasi simultaneous radio observations performed with the Green Bank (GBT) and Parkes antennas, which also constrain a Dispersion Measure of DM = 1750 ± 50 pc cm⁻³, the highest ever observed for a radio pulsar. We have found that this X-ray source is a young magnetar at ≈ 0.07 – 2 pc from Sgr A*. Simulations of its possible motion around Sgr A* show that it is likely (~90% probability) in a bound orbit around the black hole. The radiation front produced by the past activity from the magnetar passing through the molecular clouds surrounding the Galactic center region, might be responsible for a large fraction of the light echoes observed in the Fe fluorescence features.

Subject headings: X-rays: individual (SGR J1745–2900) — stars: neutron — Galaxy: center

1. INTRODUCTION

Among the large variety of Galactic neutron stars, magnetars constitute the most energetic and unpredictable class (Mereghetti 2008). They are X-ray pulsars rotating at relatively long periods (0.3–12 s, with $\dot{P} \sim 10^{-15}$ – 10^{-10} s s⁻¹), and persistent X-ray luminosities of $L_{\rm X} \sim 10^{33}$ – 10^{35} $erg s^{-1}$. They exhibit flaring activity, generally classified as giant flares ($\sim 10^{46}$ – 10^{47} erg emitted in several minutes), intermediate flares (10⁴²-10⁴⁵ erg in a few minutes) or short

- ¹ Institute of Space Sciences (CSIC-IEEC), Faculty of Science, Campus UAB, Torre C5-parell, 2a planta, 08193, Bellaterra (Barcelona), Spain
 - ² INAF IASF, Milano, via E. Bassini 15, I-20133 Milano, Italy
- ³ Departament de Fisica Aplicada, Universitat d'Alacant, Ap. Correus 99, 03080 Alacant, Spain
- Dipartimento di Fisica e Astronomia, Università di Padova, via F. Marzolo 8, I-35131 Padova, Italy
 - MSSL-UCL, Holmbury St. Mary, Dorking, Surrey RH5 6NT, UK
 - ⁶ ICREA, Barcelona, Spain
 - ⁷ INAF OAR, via Frascati 33, I-00040 Monteporzio Catone, Italy
 - 8 INAF OAC, loc. Poggio dei Pini, strada 54, I-09012 Capoterra, Italy
 - ⁹ JILA, University of Colorado, Boulder, CO 80309-0440, USA
- ¹⁰ Max Planck Institute fur Extraterrestriche Physik, D-85748 Garching, Germany
- ¹¹ Kavli Institute for Astrophysics and Space Research, Massachusetts Institute of Technology, Cambridge, MA 02139, USA
- 12 Center for Interdisciplinary Exploration and Research in Astrophysics, Physics and Astronomy Department, Northwestern University, 2145 Sheridan Rd, Evanston, IL 60208, USA

 ¹³ National Radio Astronomy Observatory, Green Bank, WV 24944,
- USA

 14 IUSS, Piazza della Vittoria 15, I-27100 Pavia, Italy
 - ¹⁵ INFN, Sezione di Pavia, via A. Bassi 6, I-27100 Pavia, Italy
- 16 Instituto de Astrofísica de Andalucía (CSIC), Glorieta de la Astronomia S/N, E-18008 Granada, Spain
 - ¹⁷ INAF IAPS, via del Fosso del Cavaliere 100, I-00133 Roma
 - ¹⁸ University of Zielona Góra, Lubuska 2, 65-265, Zielona Góra, Poland
- ¹⁹ AIM (CEA/DSM-CNRS-Université Paris Diderot), Irfu/Service d'Astrophysique, Saclay, F-91191 Gif-sur-Yvette, France.

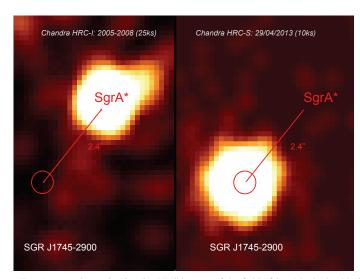
X-ray bursts $(10^{38}-10^{40} \text{ erg in less than a second})$, as well as large increases of the persistent flux (outbursts) which can last about 1 yr (Rea & Esposito 2011). The powerful emission observed from these objects has been attributed to their exceptionally high magnetic field ($B \sim 10^{14} - 10^{15} \, \mathrm{G}$ at the star surface), hence the name magnetars (Duncan & Thompson 1992; Thompson & Duncan 1993).

Analysis of stellar orbits has demonstrated that a supermassive black hole (SMBH) of about $4.3 \times 10^6 \ M_{\odot}$ resides at the dynamic center of our Galaxy (Ghez et al. 2008; Gillessen et al. 2009). The black hole is associated with Sgr A*, a compact source with non-thermal emission in radio, infrared, and X-rays (Melia & Falcke 2001; Baganoff et al. 2003; Genzel et al. 2010). X-ray fluorescence lines from numerous molecular clouds near the Galactic center have been interpreted as evidence of interaction with a light echo tracing a past bright state of Sgr A* (Ponti et al. 2013).

On 2013 April 24, Swift detected powerful X-ray emission from the direction of Sgr A* (Degenaar et al. 2013; Kennea et al. 2013), initially interpreted as an X-ray flare from the SMBH. One day later, a short X-ray burst was observed from a position consistent with that of Sgr A*, very similar in fluence, duration and spectrum to those commonly observed from magnetars. The magnetar picture received further support when NuSTAR observed the region, and detected a persistent source with periodic modulation at 3.76 s (Mori et al. 2013), a typical value for magnetar spin periods.

In this Letter we report on X-ray (Chandra and Swift) and radio (Robert C. Byrd Green Bank Telescope (GBT) and Parkes Radio Telescope) observations of SGR J1745–2900. which point to a likely physical connection of the source with $\operatorname{Sgr} A^*$.

2 Rea et al.



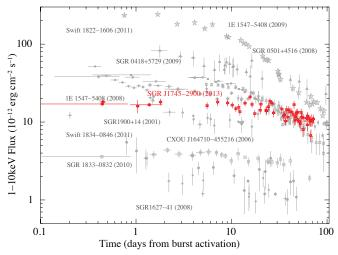


FIG. 1.— *Left panel: Chandra* HRC images of the field of Sgr A* obtained before (co-adding all previous observations performed with the HRC camera) and four days after (on 2013 April 29) the onset of the outburst of SGR J1745–2900. *Right panel: Swift/*XRT long-term flux evolution of SGR J1745–2900 in the 1–10 keV band (red squares) compared to other magnetar outbursts (adapted and updated from Rea & Esposito (2011)).

Chandra (Weisskopf et al. 2003) observed SGR J1745–2900 for the first time on 2013 April 29 with the High Resolution Camera (HRC-S), and three other times in the following three months with the Advanced CCD for Imaging Spectrometer (ACIS-S; see Table 1). The HRC-S instrument (timing mode with a 0.14" pixel size) observed SGR J1745–2900 for about 10 ks. The three ACIS-S observations were performed in faint data mode with the 1/8 chip sub-array (the source was positioned in the back-illuminated ACIS-S3 CCD at the nominal target position; time resolution 0.441 s). The data were reduced following standard procedures using the *Chandra* Interactive Analysis of Observations software (CIAO, version 4.5) and the calibration database CALDB 4.5.6.

After the discovery of SGR J1745–2900, *Swift* observed its field almost daily (see also Degenaar et al. (2013); Kennea et al. (2013)). In this work we use all the observations performed between TJD 16406 and 16480, taken in both photon counting (PC) and windowed timing (WT) modes. Only the WT observations could be used for the timing analysis of SGR J1745–2900 (Section 2.2; readout time of 1.7 ms), owning to the slow read out time of the PC mode (2.5 s). The data were processed and filtered with standard criteria using Ftools within HEAsoft software package (v6.12).

For the ACIS observation, the spectra, ancillary response files and spectral redistribution matrices were created using the CIAO script specextract. For the XRT observations, we used the latest available spectral redistribution matrix in CALDB (v013/v014), while the ancillary response files were generated with xrtmkarf, and they account for different extraction regions, vignetting and PSF corrections.

We have converted all photon arrival times to the Barycentric Dynamical Time (TDB) system, using the accurate position derived from the *Chandra* observations (see below).

2.1. Absolute astrometry

In the ACIS-S observations a number of sources were detected besides SGR J1745–2900. In particular, four known sources present in an X-ray catalog (Muno et al. 2009) were located within $\sim 30''$ from the SGR and could be employed to

refine the absolute astrometry. We used the four source positions, calculated with wavdetect, to register the ACIS-S images on the catalog by optimizing a roto-translation (using the CIAO script reproject_aspect). The fit yielded an average rms of $\sim\!80$ mas. The estimated coordinates (taking into account also the accuracy of the reference positions) of SGR J1745–2900 are: RA = $17^{\rm h}45^{\rm m}40^{\rm s}.169$, Dec = $-29^{\circ}00'29'.84$ (J2000.0) with a 95% confidence level uncertainty radius of 0'.3 (see Fig. 1).

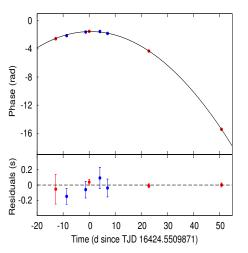
2.2. X-ray timing analysis

Because of the complex shape and variability of the three peaked pulse profile (Fig. 2), we decided not to use a pulse template for the timing analysis (which might artificially affect the phase shift), using instead two parallel methods: fitting a sinusoid to the profile at the fundamental period, and fitting the highest peak in all the observations with a Gaussian. We used 12 phase bins to produce a folded pulse profile. We built up our timing solution from the phases of the second *Chandra* pointing which has the highest number of counts. The resulting best-fit period for this *Chandra* observation was P = 3.763554(2) s (at TJD 16424.5509871; TJD = JD - 2440000.5 days). The accuracy on this measure of the period, 2 μ s, is enough to coherently phase-connect adjacent observations. At each step, we checked that the timing solution was accurate enough to determine univocally the phase of the following observation. To this end, we propagated the error affecting the best-fitting parameters of the solution obtained at any step, to the epoch of the newly added observation. We never obtained a phase uncertainty larger than 0.4, which allowed us to tentatively maintain the phase connection. The phase-coherent solution obtained considering the phases of the best-fit fundamental harmonic component has a period P = 3.7635537(2) s and period derivative $\dot{P} = 6.61(4) \times 10^{-12} \,\mathrm{s \ s^{-1}}$ (epoch TJD 16424.5509871), with a reduced chi-squared of 0.85 for 5 degrees of freedom (dof). On the other hand, when comparing this results with the timing solution derived considering the phases of the best-fit Gaussian to the main peak, we find compatible

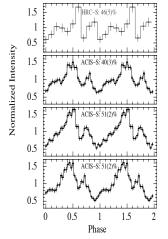
	Chana	dra X-ray observations)
Obs. ID (Instrument)	Start date	Count-rate	Exposure	1-10 keV Flux
	(yy-mm-dd hh:mm:ss)	(counts/s)	(ks)	$(10^{-12} \mathrm{erg} \mathrm{s}^{-1} \mathrm{cm}^{-2})$
14701 (HRC-S)	2013-04-29 15:19:50	0.087(2)	9.8	-
14702 (ACIS-S)	2013-05-12 10:45:41	0.383(5)	15.1	9.2(3)
14703 (ACIS-S)	2013-06-04 08:45:16	0.310(4)	16.8	7.3(2)
14946 (ACIS-S)	2013-07-02 06:57:56	0.274(4)	18.2	6.3(2)
	R	adio observations)
Telescope (Backend)	Start UT Time	Frequency (Bandwidth)	Length	Flux
	(yy-mm-dd hh:mm:ss)	MHz (MHz)	(ks)	(mJy)
PKS (PDFB4)	2013-04-27 13:53:04	3094 (1024)	5.4	< 0.02
PKS (PDFB4)	2013-04-28 15:21:34	3094 (1024)	1.2	< 0.05
GBT (GUPPI)	2013-04-29 07:14:54	2000 (800)	1.5	< 0.02
PKS (PDFB4)	2013-04-29 16:27:38	3094 (1024)	5.4	0.06
PKS (PDFB4)	2013-05-01 14:45:01	3094 (1024)	1.2	0.1

8900 (800)

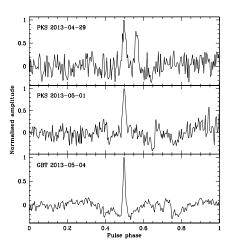
 $TABLE\ 1 \\ JOURNAL\ OF\ THE\ \emph{Chandra},\ GREEN\ BANK\ AND\ PARKES\ OBSERVATIONS.$



GBT (GUPPI)



2013-05-04 11:35:13



0.04

FIG. 2.— Left panel: evolution of the rotational phase and the residuals with respect to the timing solution reported in the text ($\S 2.2$; in red the Chandra observations and in blue the Swift ones). Middle panel: Pulse profiles of the four Chandra observations with the relative pulsed fraction (defined as (Max – Min)/(Max + Min) of the pulse profile). Right panel: Pulse profiles of the three radio observations where the magnetar was detected (see $\S 3$ and Table 1).

numbers for the period and the period derivative, but with a marginal evidence for a cubic component (resulting in a possible $|\ddot{P}| = 4(3) \times 10^{-19} \, \mathrm{s \, s^{-2}}$).

2.3. X-ray spectral analysis

In the *Chandra* observations, the pileup in the ACIS-S3 detector was $\sim 5-15\%$, therefore an annular region with 0.75'' inner radius (1.5 pixels) and 2'' outer radius was selected to extract the source spectrum. For the background we used an annular region of maximum radius 8'' around the source. The point source spectrum was rebinned to have at least 50 counts per energy bin.

We modeled the spectra using the XSPEC v.12.8.0j analysis package. An absorbed single blackbody component (BB) provides a good fit to the data of the three ACIS–S observations ($\chi_r^2 \sim 1.13$ with 313 dof); the best-fit parameters are: $N_{\rm H} = 1.03(4) \times 10^{23} \, {\rm cm}^{-2}$ (abundances and cross-section from Anders & Grevesse (1989) and Balucinska-Church & McCammon (1998)), with a temperature cooling from $kT = 0.95(2) \, {\rm keV}$, to $kT = 0.90(2) \, {\rm keV}$ and then $kT = 0.88(2) \, {\rm keV}$ for the three observations, respec-

tively. The blackbody radius remains constant within errors at $R_{\rm BB} \simeq 1.4\,$ km (assuming a 8.3 kpc distance). The 1–10 keV source flux (see Table 1) corresponds to a luminosity of 2.1, 1.8 and $1.6 \times 10^{35} {\rm erg \, s^{-1}}$ (assuming a 8.3 kpc distance).

However, we note that the fit residuals are not optimal at higher energies, possibly due to the presence of a non-thermal component. By fitting with a power-law function we also obtain a good modelling ($\chi^2_r \sim 1.04$ with 313 dof), with $N_{\rm H}=1.73(4)\times 10^{23}\,{\rm cm}^{-2}$, with photon index of $\Gamma=3.9(1)$, 4.1(1) and 4.2(1) for the three observations. The residuals are slightly better shaped at higher energy. A composition of a blackbody plus power-law model is not statistically required by the data, and does not improve the fit.

The X-ray flux decay can be modeled with an exponential function of the form $F(t) = F_{\circ} e^{(-(t-t_{\circ})/\tau)}$ ($\chi^2_{\nu} = 1.44$ for 80 dof). We fixed t_{\circ} at the time of the first burst detected; the resulting best-fit parameters are $F_{\circ} = 1.72(3) \times 10^{-11}$ erg cm⁻² s⁻¹ and e-folding time $\tau = 144(8)$ days. This is a rather slow flux decay as compared with other outbursts (Fig. 1).

3. RADIO OBSERVATIONS

4 Rea et al.

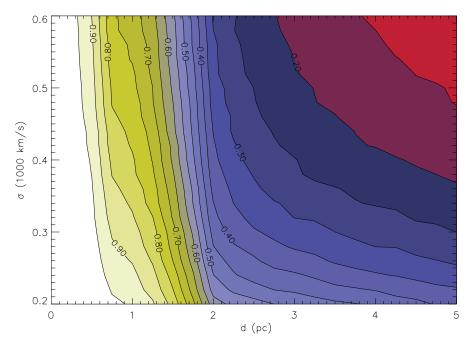


FIG. 3.— Probability for SGR J1745-2900 to be in a bound orbit around the Galactic center SMBH obtained from Monte Carlo simulations (see text for details).

We have also started a monitoring campaign in the radio band using the 64-m Parkes (NSW, Australia) and the 100m GBT (WV, USA) radio telescopes to study the magnetar's radio emission (Eatough et al. 2013). Given the very high electron column density expected in the central regions of the Galaxy we chose to observe at 3.1 GHz (over a bandwidth of 1024 MHz split into 512 frequency channels) at Parkes, and at 2 and 8.9 GHz (with a bandwidth of 800 MHz split into 2048 frequency channels) at GBT (see Table 1). At Parkes observations were performed using the ATNF digital filterbank (DFB4; Ferris & Saunders (2004)) in search mode, 2-bit sampling the data every 125 μ s, while at GBT the Green Bank Ultimate Pulsar Processing Instrument (GUPPI; DuPlain et al. (2008)) was used in search mode, 8-bit sampling the data every 64 μ s. For a faster analysis, GBT data were downsampled in time by a factor of 4 and in frequency by a factor of 8. Data show that at 2–3 GHz, the magnetar switched on between 2013 April 28 and 29. During the Parkes observation the magnetar pulse profile showed a two peaks profile, that evolved into a single one in all subsequent detections (Fig. 2). From the 10-cm Parkes observations, we obtained a dispersion measure DM = 1750 ± 50 pc cm⁻³ measured using the Tempo2 software package (consistent with the value derived by Eatough et al. (2013); Shannon & Johnston (2013)).

4. DISCUSSION

We performed a series of *Chandra* observations of the Galactic center, determing the position of a new transient magnetar in the crowded region of Sgr A* (see Fig. 1). SGR J1745–2900 is at an angular distance from the position of Sgr A* (Petrov et al. 2011) of only 2.4 ± 0.3 arcsec. The timing parameters derived in section §2.2, imply a surface dipolar magnetic field at the equator $B_{\rm p}\sim3.2\times10^{19}\sqrt{P\dot{P}}\,{\rm G}=1.6\times10^{14}\,{\rm G},$ a rate of rotational energy loss $\dot{E}\sim3.9\times10^{46}\dot{P}/P^3\,{\rm erg\,s^{-1}}=4.9\times10^{33}{\rm erg\,s^{-1}},$ and a characteristic age $\tau_c\sim P/(2\dot{P})\sim9\,{\rm kyr}.$

Radio observations performed with Parkes and GBT detected the magnetar radio emission (Eatough et al. 2013), with the flux and pulse profile variability typical of radio magnetars. The dispersion measure derived from Parkes observations at $10 \, \mathrm{cm}$, $DM = 1750 \pm 50 \, \mathrm{pc \, cm^{-3}}$, is the highest ever measured for a radio pulsar, and implies a distance of $\sim 8.3 \, \mathrm{kpc}$ (Cordes & Lazio 2002). The relatively high $\dot{E} \sim 5 \times 10^{33} \, \mathrm{erg \, s^{-1}}$ of SGR J1745–2900 compared with the deep limit of its quiescent emission derived by several Ms of *Chandra* observations ($\sim 10^{32} \, \mathrm{erg \, s^{-1}}$ in the 2–10 keV range; Muno et al. (2005)) supports the predictions of the fundamental plane for radio magnetars (Rea et al. 2012).

4.1. Association between SGR J1745-2900 and Sgr A*

The difference between the column densities of SGR J1745–2900 (see section §2.3) and SgrA* (Baganoff et al. 2003) translates into $|N_{\rm H,\,J1745}-N_{\rm H,\,SgrA^*}|\lesssim 0.6\times 10^{23}{\rm cm}^{-2}$ (at 90% confidence level). Given that the Central Molecular Zone (CMZ) has a particle density $N_{\rm CMZ}>10^4{\rm\,cm}^3$ (Morris & Serabyn 1996), this yields an upper limit on the distance between the two sources $d_{\rm max}=|N_{\rm H,\,J1745}-N_{\rm H,\,SgrA^*}|/N_{\rm CMZ}\sim 2\,{\rm\,pc}$.

 $d_{\rm max}=|N_{\rm H,\;J1745}-N_{\rm H,\;SgrA^*}|/N_{\rm CMZ}\sim 2\;{\rm pc}.$ SGR J1745–2900 and Sgr A* relative distance ranges between that implied by their angular separation on the sky, $d_{\rm min}=0.09\pm0.02\,{\rm pc},$ and $d_{\rm max}\sim 2\,{\rm pc}.$ With an estimated neutron star density in the Galactic disc $\approx 3\times 10^{-4}\;{\rm pc}^{-3}$ (Faucher-Giguère & Kaspi 2006), we expect ~ 0.2 neutron stars in a cone of aperture 2".4 which encompasses the Galactic Center, and reaches out to the rim of the Galaxy (assumed distance from the Sun is 20 kpc). This estimate comprises all neutron stars born during the Galaxy lifetime, in about 1 Gyr. The probability of SGR J1745–2900 being a neutron star wandering across the line of sight, with an age $\lesssim 9\,{\rm kyr},$ and lying at such a small angular distance from Sgr A* is then $\sim 1.8\times 10^{-6}$. This makes the possibility that SGR J1745–2900 is a foreground or background object quite unlikely.

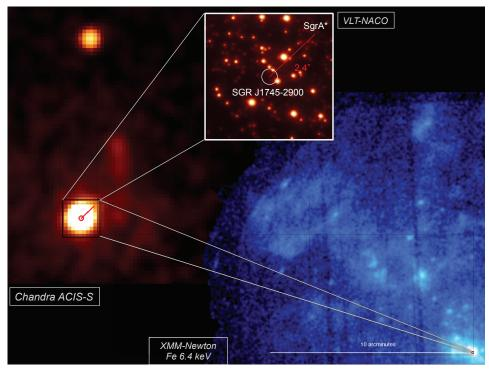


FIG. 4.— Multiwavelength view of the field of SGR J1745–2900 and Sgr A*. The blue image shows the XMM-Newton 6.4 keV Galactic center view (Ponti et al. 2013), and the black square reports a $5'' \times 5''$ box around the position of the magnetar. The inset shows our first *Chandra* ACIS observation. We also show the dense massive star population as observed by VLT/NaCo in the near-infrared K_s band (Schödel et al. 2009).

On the other hand, estimates of the neutron star population in the Galaxy (Freitag et al. 2006) suggest that there are about 2×10^4 neutron stars within 1 pc from the Galactic center. Since this is the total population born during the entire lifetime of the Galaxy (about a Gyr), a new neutron star is born in the same region every $\sim 10^5$ yr. Even on an observational ground alone, about 80 ordinary radio pulsars (Wharton et al. 2012) are expected to be visible with 1 pc from Sgr A*, compatible with us seeing only one young radio pulsar with a characteristic age $<\!10\,\mathrm{kyr}$. The magnetar nature of this young radio pulsar so close to Sgr A* suggests that there might possibly be as many magnetars as ordinary pulsars in the Galaxy (Rea et al. 2010), and/or the Galactic center region is a favorable place for magnetar formation, possibly because of its high density of very massive stars.

The projected position of SGR J1745–2900 places it within the disk of young and massive stars observed within 0.5 pc of Sgr A* (Paumard et al. 2006; Lu et al. 2009), which is most likely its birthplace (see Fig. 4). SGR J1745–2900 is probably the end product of one of the young massive stars born during a recent star formation activity within the dense gaseous disk around Sgr A*, now accreted into the black hole (Levin & Beloborodov 2003).

The probability of SGR J1745–2900 being in a bound orbit around Sgr A* depends on the distance and the kick velocity of the neutron star at birth. In order to estimate the probability that SGR J1745–2900 is in a bound orbit around Sgr A*, we performed numerical simulations by integrating the equations of motion in the gravitational potential of the central black hole for a large number ($\sim 10^6$) of stars; Newtonian gravity was assumed throughout. For each orbit the initial radial distance d (0.05 pc $\leq d \leq$ 5 pc) was fixed and the star position on the sphere was selected by generating two uniform deviates. The modulus of the initial velocity was drawn from a Gaussian distribution with specified standard

deviation σ (200 km s⁻¹ $\leq \sigma \leq$ 600 km s⁻¹); the velocity direction was determined by generating two further uniform deviates. Orbits were calculated in the time interval $0 \le t \le T$, where T = 9 kyr is the estimated age of SGR J1745–2900. Stars which at t = T are at a projected radial distance of 0.07-0.11 pc are sorted according to the value of their total energy, E. Finally the fraction of bound orbits is computed as $N(E < 0)/N_{tot}$. Since a large number of runs are required to explore with sufficiently small uncertainties the d and σ ranges, we resorted to a 2D model, in which orbits are in the plane of the sky only. We checked that results from the 2D calculations are in good agreement with those of the complete 3D case for the present purposes. The Monte Carlo simulations are summarized in Fig. 3, that shows the fraction of bound orbits as a function of d and σ : if the magnetar was born within 1 pc of Sgr A* (where most of the massive stars are located) the probability of being in a bound orbit around the black hole is \sim 90%. For a circular orbit of radius 0.1 pc, the orbital period would be 1430 yr, while the minimum orbital period would be 500 yr with the pulsar being now at the apastron of a strongly eccentric orbit (Liu et al. 2012). Orbital periods for different eccentricities and semi-major axes can reach periods of several kyrs.

4.2. The possible imprint of SGR J1745–2900's past activity on the Galactic center Fe fluorence

Studies of the Galactic center environment led to the discovery of Fe K α emission (Koyama et al. 1997) from molecular clouds within ${\sim}300\,\mathrm{pc}$ from Sgr A* (Fig. 4). The fast variability of these Fe emission features (Ponti et al. 2010; Clavel et al. 2013) supports an interpretation in terms of irradiation from one or more radiation fronts passing through the different molecular clouds in the Galactic Center, emitted ${\sim}100\,\mathrm{yr}$ ago. The luminosity needed to explain the Fe fluorescence can be calculated as $L_{\rm 8keV} \sim 6 \times 10^{38} \times f \,\mathrm{erg}\,\mathrm{s}^{-1}(\mathrm{Sunyaev}\,\&$

6 Rea et al.

Churazov 1998), where f is a parameter taking into account flares with duration Δt shorter than the cloud light-crossing time: $f \simeq (R_{\rm cloud}/c)/\Delta t$. The total required fluence is then $\approx L_{8\,\mathrm{keV}} \times T_{\mathrm{echo}} \sim 10^{46} \text{--} 10^{47} \,\mathrm{erg}$, where $T_{\mathrm{echo}} \approx 1 \text{--} 10 \,\mathrm{yr}$ is the light crossing time of the fastest echoing clouds (Clavel et al. 2013). This energy could have been emitted by a powerful giant flare (similar to the one observed from SGR 1806-20; Hurley et al. (2005)) from SGR J1745–2900 about a century ago. Unfortunately a reliable measure of the soft X-ray flux of the peak of SGR 1806–20's giant flare is not available (Hurley et al. 2005; Inan et al. 2007), however for the SGR 1900+14's giant flare the study of the ionosphere disturbance could give an estimate of its 3–10 keV flux as a factor of ~ 9 times the hard X-ray emission level (Inan et al. 1999). This is also in line with the idea of the softer component being due to the thermal emission from an expanding fireball, which in smaller scale bursts are observed to have a spectrum consistent with a blackbody with $kT \sim 7-10$ keV. The non-thermal hard X-ray emission during the flare peak is instead due to non-thermal processes deriving from the particle acceleration caused by the fireball. The > 50 keV peak flux of SGR 1806-20's giant flare was estimated to be \sim 20 erg s⁻¹cm⁻²by GEOTAIL measurements (the only instrument providing a good estimate of the first <1 s flare flux; Terasawa et al. (2005)). Assuming a distance of 15 kpc (McClure-Griffiths & Gaensler 2005), this translates in a luminosity (>50 keV) of $\sim 5 \times 10^{46} {\rm erg \, s}^{-1}$. A good guess of the 3-10 keV emission during the SGR 1806-20's giant flare would then be about an order of magnitude higher luminosity, large enough to be the cause (or a substantial part) of the photon flux responsible for the observed Fe emission. Furthermore, the requirement that a very energetic event from SGR J1745-2900 occurred ~100 yr ago is compatible with the estimated outburst rate of a magnetar with such properties, which is approximately one every 50–100 yrs (Viganò et al. 2013; Perna & Pons 2011).

5. CONCLUSIONS

SGR J1745–2900 is the first pulsar discovered at a parsec distance from a supermassive black hole with a non-negligible probability of being in a bound orbit. Future measurements of the magnetar proper motion and, possibly, spin-down variability (the contribution to the magnetar observed \dot{P} due to the acceleration imparted by Sgr A*'s gravitational well can be up to $\sim 8 \times 10^{-13} \ s \ s^{-1}$), will be key in observing the effects of the supermassive black hole's gravitational potential on the magnetar's evolution.

We thank the Chandra team, director and Scott Wolk, for the extremely efficient work, and Ryan Shannon for carrying out some of the Parkes observations. NR thanks Giovanni Miniutti and Kevin Hurley for useful discussion. The National Radio Astronomy Observatory is a facility of the National Science Foundation operated under cooperative agreement by Associated Universities, Inc. . The Parkes radio telescope is part of the Australia Telescope which is funded by the Commonwealth of Australia for operation as a National Facility managed by CSIRO. We acknowledge support by grants AYA 2012-39303, SGR2009-811, iLINK 2011-0303, AYA 2010-21097-C03-02, Prometeo 2009/103, AYA2010-17631, P08-TIC-4075, INAF 2010 PRIN grant, Chandra Awards GO2-13076X, G03-14060X, GO3-14099X and G03-14121X, and an EU Marie Curie IEF (FP7-PEOPLE-2012-IEF-331095).

REFERENCES

Anders, E. & Grevesse, N., 1989, Geochimica et Cosmochimica Acta 53, Baganoff, F. K., Maeda, Y., Morris, M., et al. 2003, ApJ, 591, 891 Balucinska-Church, M. & McCammon, D., 1998, ApJ, 496, 1044 Clavel, M., Terrier, R., Goldwurm, A., et al. 2013, arXiv:1307.3954 Cordes, J. M. & Lazio, T. J. W. 2002, eprint (astro-ph/0207156) Degenaar, N., Miller, J. M., Kennea, J., et al. 2013, ApJ, 769, 155 Duncan, R. C. & Thompson, C. 1992, ApJ, 392, L9 DuPlain, R., Ransom, S., Demorest, P., et al. 2008, Proc. SPIE, 7019, Eatough, R., et al., 2013, Atel #5040 Faucher-Giguère, C.-A. & Kaspi, V. M. 2006, ApJ, 643, 332 Ferris, R. H., & Saunders, S. J. 2004, Experimental Astronomy, 17, 269 Freitag, M., Amaro-Seoane, P., & Kalogera, V. 2006, ApJ, 649, 91 Genzel, R., Eisenhauer, F., & Gillessen, S. 2010, Reviews of Modern Physics, 82, 3121 Ghez, A. M., Salim, S., Weinberg, N. N., et al. 2008, ApJ, 689, 1044 Gillessen, S., Eisenhauer, F., Trippe, S., et al. 2009, ApJ, 692, 1075 Hurley, K., Boggs, S. E., Smith, D. M., et al. 2005, Nature, 434, 1098 Inan, U. S., Lehtinen, N. G., Moore, R. C., et al. 2007, Geophys. Res. Lett., Inan, U. S., Lehtinen, N. G., Lev-Tov, S. J., et al. 1999, Geophys. Res. Lett., 26, 3357

Kennea, J. A., Burrows, D. N., Kouveliotou, C., et al. 2013, ApJ, 770, L24 Koyama, K., Kinugasa, K., Matsuzaki, K., et al. 1997, PASJ, 49, L7 Levin, Y., & Beloborodov, A. M. 2003, ApJ, 590, L33 Liu, K., Wex, N., Kramer, M., Cordes, J. M., & Lazio, T. J. W. 2012, ApJ,

747, 1 Lu, J. R., Ghez, A. M., Hornstein, S. D., et al. 2009, ApJ, 690, 1463 Melia, F. & Falcke, H. 2001, ARA&A, 39, 309 McClure-Griffiths, N. M., & Gaensler, B. M. 2005, ApJ, 630, L161

Mereghetti, S. 2008, A&A Rev., 15, 225

Mori, K., Gotthelf, E. V., Zhang, S., et al. 2013, ApJ, 770, L23 Morris, M., & Serabyn, E. 1996, ARA&A, 34, 645

Muno, M. P., Pfahl, E., Baganoff, F. K., et al. 2005, ApJ, 622, L113 Muno, M. P., Bauer, F. E., Baganoff, F. K., et al. 2009, ApJS, 181, 110

Paumard, T., Genzel, R., Martins, F., et al. 2006, ApJ, 643, 1011 Perna, R. & Pons, J. A. 2011, ApJ, 727, L51

Petrov, L., Kovalev, Y. Y., Fomalont, E. B., & Gordon, D. 2011, AJ, 142, 35 Ponti, G., Morris, M. R., Terrier, R., & Goldwurm, A. 2013, in Astrophysics and Space Science Proceedings, Vol. 34, Cosmic Rays in Star-Forming Environments, ed. D. F. Torres & O. Reimer (Springer, Heidelberg), 331-370

Ponti, G., Terrier, R., Goldwurm, A., Belanger, G., & Trap, G. 2010, ApJ, 714 732

Rea, N. & Esposito, P. 2011, in High-Energy Emission from Pulsars and their Systems, ed. D. F. Torres & N. Rea, Astrophysics and Space Science Proceedings (Springer, Heidelberg), 247–273

Rea, N., Esposito, P., Turolla, R., et al. 2010, Science, 330, 944

Rea, N., Pons, J. A., Torres, D. F., & Turolla, R. 2012, ApJ, 748, L12

Schödel, R., Merritt, D., & Eckart, A. 2009, A&A, 502, 91

Shannon, R. M. & Johnston, S. 2013, MNRAS, submitted (eprint: astroph/1305.3036)

Sunyaev, R. & Churazov, E. 1998, MNRAS, 297, 1279

Terasawa, T., Tanaka, Y. T., Takei, Y., et al. 2005, Nature, 434, 1110

Thompson, C. & Duncan, R. C. 1993, ApJ, 408, 194

Viganò, D., Rea, N., Pons, J. A., Perna, R., Aguilera, D., & Miralles, J. A. 2013, MNRAS, 434, 123

Weisskopf, M. C., Aldcroft, T. L., Bautz, M., et al. 2003, Experimental Astronomy, 16, 1

Wharton, R. S., Chatterjee, S., Cordes, J. M., Deneva, J. S., & Lazio, T. J. W. 2012, ApJ, 753, 108